

## ***Interactive comment on “Destruction and reinstatement of coastal hypoxia in the South China Sea off the Pearl River Estuary” by Yangyang Zhao et al.***

Yangyang Zhao<sup>1,2</sup>, Khanittha Uthaipan<sup>1</sup>, Zhongming Lu<sup>3</sup>, Yan Li<sup>1</sup>, Jing Liu<sup>1</sup>, Hongbin Liu<sup>4,5</sup>, Jianping Gan<sup>3,5,6</sup>, Feifei Meng<sup>1</sup>, Minhan Dai<sup>1</sup>

<sup>1</sup>State Key Laboratory of Marine Environmental Science, Xiamen University, Xiamen, 361102, China

<sup>2</sup>Environmental Physics, Institute of Biogeochemistry and Pollutant Dynamics, ETH Zurich, Zurich, 8092, Switzerland

<sup>3</sup>Division of Environment and Sustainability, Hong Kong University of Science and Technology, Kowloon, Hong Kong SAR, China

<sup>4</sup>Division of Life Science, Hong Kong University of Science and Technology, Kowloon, Hong Kong SAR, China

<sup>5</sup>Department of Ocean Science, Hong Kong University of Science and Technology, Kowloon, Hong Kong SAR, China

<sup>6</sup>Department of Mathematics, Hong Kong University of Science and Technology, Kowloon, Hong Kong SAR, China

Correspondence to: Minhan Dai (mdai@xmu.edu.cn)

### **Anonymous Referee #1**

#### **General comments:**

*In their manuscript Zhao et al investigate the effects of a typhoon on subsurface water reoxygenation following hypoxic condition off the Pearl River Estuary and the subsequent time scale of hypoxia formation. The author calculate the oxygen consumption rate in bottom waters using a three end-member mixing model. The subject of the paper is not novel but is an interesting approach and relevant for the region and the journal. The use of the model is interesting although the assumption about the "quasi-static bottom waters" is questionable and do not seem to fit with the observations (e.g. Figure 3, see specific comments below). The observations and analysis are fine but too limited to fully support the conclusions. The authors rely heavily on the literature, whereas they could provide analysis or observations to support their interpretations. For example it would be interesting to see a sequence of oxygen vertical profiles, at multiple locations, when they look into the time-scale of hypoxia development after the typhoon. Volume might be an important factor at this time, although it is not mentioned because, as I understand, OCR is assumed to be uniform in subsurface waters. Does that imply that sediment oxygen demand is negligible? DIC observations are not used presently, although their analysis could strengthen the conclusions by relating OCR with respiration. Finally, part of the Discussion is a review of the literature (e.g. section 4.3) that is interesting but somewhat disconnected from the results presented. The discussion about hypoxia under future climate is highly hypothetical. Overall, the manuscript provides interesting results but could be significantly improved with more in-depth analyses of the observations. The quality of some figures could also be improved. Detailed comments are listed below.*

**[Response]:** We appreciate the critical and constructive comments from the reviewer. The reviewer is correct that bottom waters may be dynamic upon disturbance by typhoon as reflected notably in vertical mixing. Here our "quasi-static bottom waters" assumption was referring to the limited exchanges between the oxygen-depleted bottom water mass under study with the surrounding environment. More specifically, we contend that this assumption was reasonable for calculating the oxygen consumption rate (OCR) from Leg 2 to Leg 3 because hypoxic zones are typically developed in strong convergent zones (Lu et al. 2018; Li et al. 2020) with thus longer residence time that facilitates oxygen consumption. Indeed, the bottom water residence time in the sampling area was ~ 15 days (Li et al. 2020), significantly longer than the time lag from Leg 2 to Leg 3 (~ 6 days). We thus contend that the disturbance by typhoon mainly led to vertical mixing instead of horizontal water mass exchanges. The upward-intruded bottom waters were indeed visible in the time-series observations, and such vertical mixing was gradually suppressed by the surface plume-induced stratification (Fig. 1). The water column below the pycnocline became almost vertically well-mixed to the end of the time-series observations before Leg 2. Based on the above notions and the reviewer's comments, we will revise our assumption as "the bottom water masses where biochemical oxygen-consumption significantly took place were constrained by strong convergence and their outflow from the sampling area is insignificant on the time scale of the water residence time" in our revised manuscript.

The reviewer is also correct that the OCR was assumed to be uniform in the subsurface waters, because (1) we only collected samples at three depth layers during Leg 2 and Leg 3, with usually only one depth layer below the pycnocline; (2) if the middle layer was below the pycnocline, the concentration of dissolved oxygen (DO) almost equaled to that at the bottom layer (e.g., Station F304; Fig. 3k). Sediment oxygen demand might be significant near the seabed or in its overlying water column (Kemp et al. 1992, Zhang and Li 2010), but in our sampling area Cui et al. (2019) found much smaller oxygen losses by sediment oxygen demand (i.e., benthic respiration) than the bacterial respiration in the water column based on both incubation experiments and oxygen budget analysis. We thus assumed the sediment oxygen demand was negligible and the microbial respiration in the water column dominated the estimated OCR.

We agree with the reviewer that we should fully use our data to support our conclusions. Besides using dissolved inorganic carbon (DIC) and total alkalinity (TA) to validate our three-

endmember mixing model, we have further calculated the biochemical-induced DIC changes from Leg 2 to Leg 3 and showed its relationship to the biochemical-induced DO changes, with a slope of  $-0.92 \pm 0.17$  (Fig. 2), implying aerobic respiration dominated the OCR. We must point out that we did not directly estimate the DIC production rate, because uncertainties in DIC from the conservative mixing among three water masses reached  $\sim 30 \mu\text{mol kg}^{-1}$ , comparable to changes in DIC between two legs for nearly half of the sampling stations during Leg 3. We have however further added the oxygen profiles at multiple stations clearly showing their temporal variations (Fig. 3): the DO concentration below the pycnocline significantly decreased from Leg 2 to Leg 3 and was almost homogeneous vertically.

We also agree with the reviewer that some part of the discussions was disconnected to our results and estimates. We will thus reorganize our paper to combine results and discussion into a clear narrative, with an outline as below:

### 3 Evolution of intermittent hypoxia off the PRE

#### 3.1 Extensive hypoxia before typhoon

#### 3.2 Destruction of hypoxia by typhoon

#### 3.3 Reinstatement of hypoxia after typhoon

### 4 Maintenance, destruction and reinstatement of coastal hypoxia

#### 4.1 Water column stability

#### 4.2 Oxygen sinks and hypoxia formation timescale

##### 4.2.1 Mixing-induced oxygen sinks

##### 4.2.2 Biochemical-induced oxygen sinks

##### 4.2.3 Hypoxia formation timescale

#### 4.3 Imprint of tropical cyclones on the evolution of coastal hypoxia

In particular, we will further modify the discussions on (1) the tidal effects on hypoxia by calculating the potential maximum hypoxic area, as spring-to-neap tidal oscillations lead to variations in the DO concentration with a maximum neighboring oxygen range of  $0.5 \text{ mg L}^{-1}$  (Cui et al. 2019); and (2) the effect of tropical cyclones-induced processes on the restoration of hypoxia and the response of the hypoxia's evolution to the changes in the frequency and intensity of tropical cyclone activities, based on our observations of post-storm stronger blooms and additional statistics of annual mean number and wind direction of tropical cyclones and the time interval between two successive tropical clones (Fig. 4 and Table 1).

We have also improved the quality of the figures by splitting the figure showing spatial distributions of temperature, salinity, DO and chlorophyll *a* (Chl *a*) concentrations into two figures, enlarging labels and adding additional information. We will further address these concerns from the reviewer in our responses as of below.

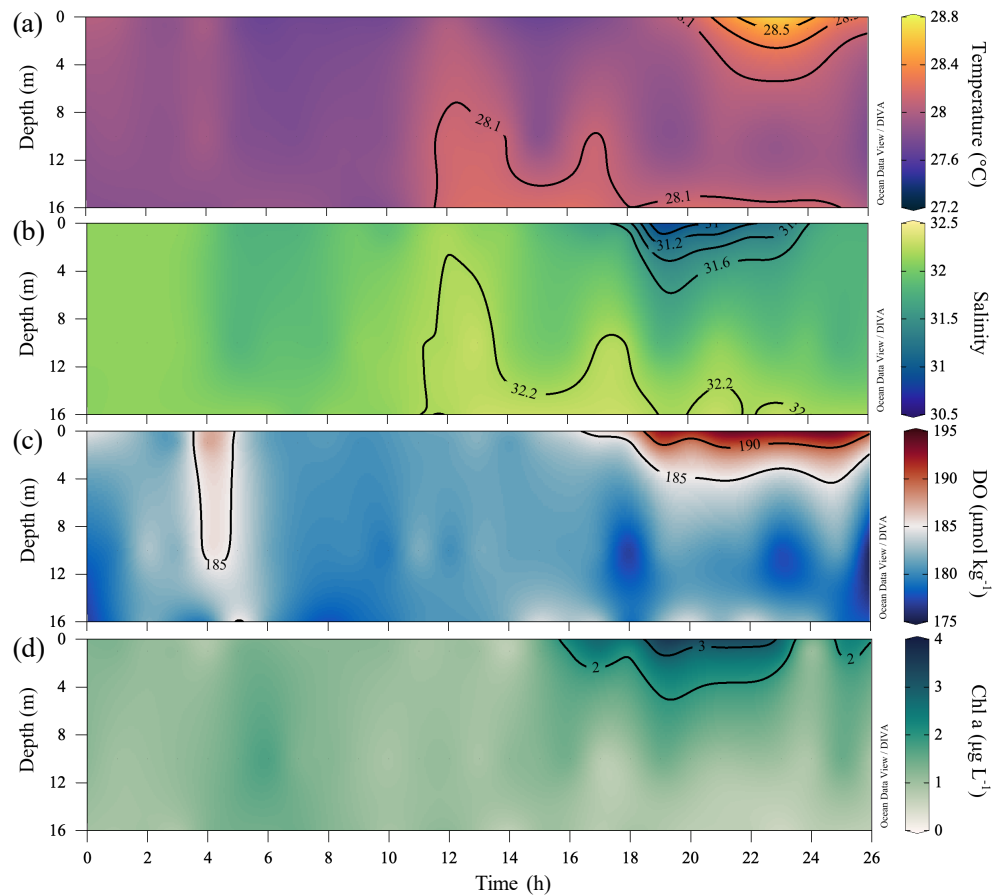


**Figure 1 :** Time-series distribution of (a) temperature (°C), (b) salinity, (c) DO ( $\mu\text{mol kg}^{-1}$ ) and (d) Chl *a* concentrations ( $\mu\text{g L}^{-1}$ ) at Station F303 (see Fig. 1b) from July 19-20, 2018, post typhoon passage, showing the complete destruction and the subsequent rapid development of stratification.

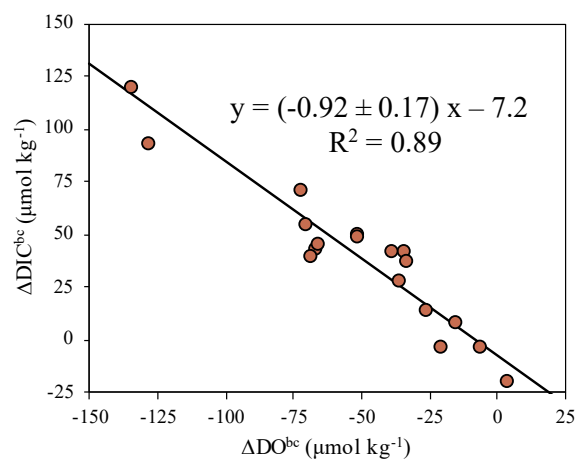


**Figure 2:** The biochemical-induced changes in DIC ( $\Delta\text{DIC}^{\text{bc}}$ ,  $\mu\text{mol kg}^{-1}$ ) vs. DO ( $\Delta\text{DO}^{\text{bc}}$ ,  $\mu\text{mol kg}^{-1}$ ) in bottom waters with depths  $> 10$  m from Leg 2 to Leg 3. The black line denotes the slope of  $\Delta\text{DIC}^{\text{bc}}$  plotted against  $\Delta\text{DO}^{\text{bc}}$  derived from the Model II regression.

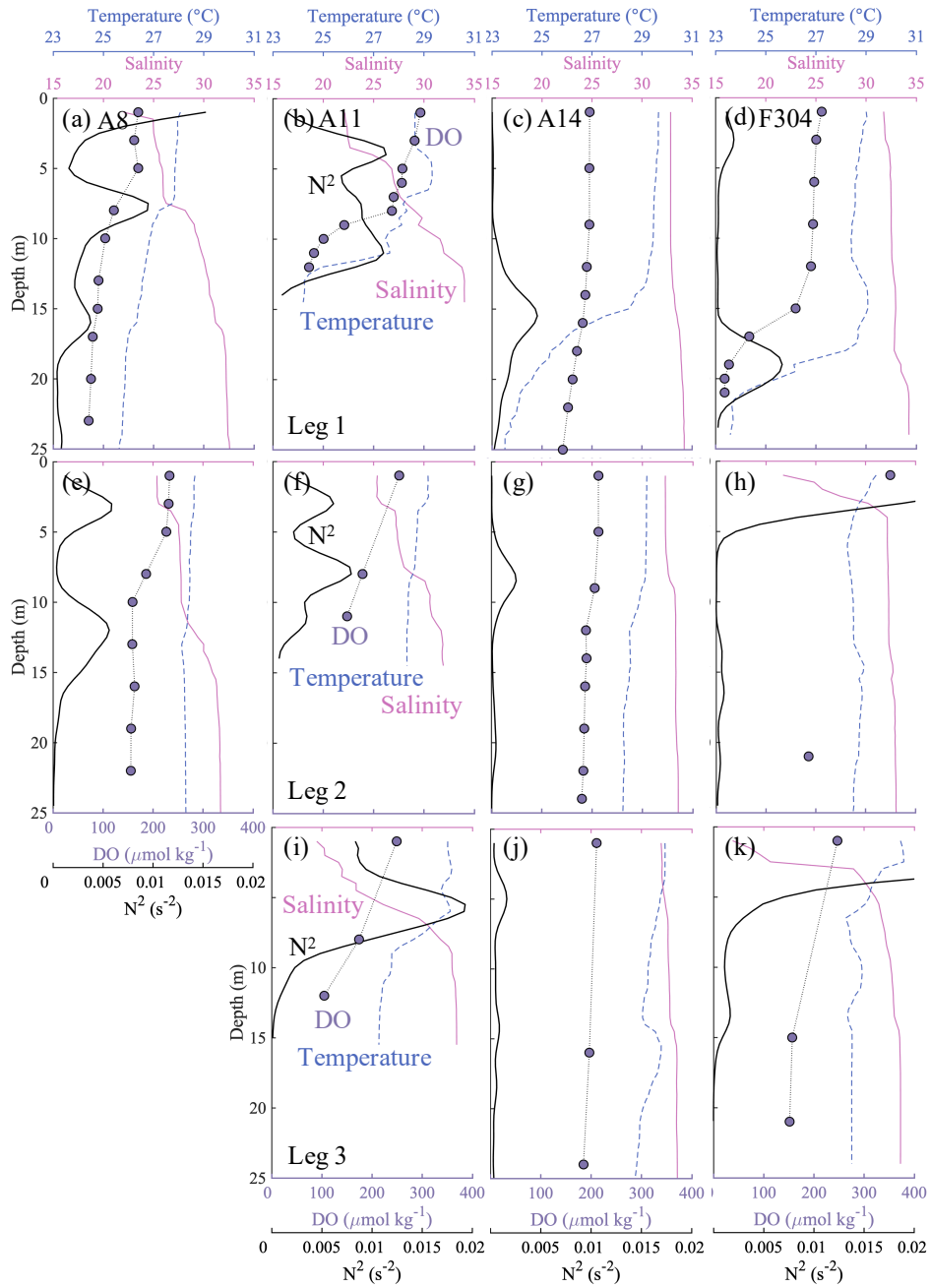


**Figure 3:** Profiles of temperature ( $^{\circ}\text{C}$ ) (green dashed lines), salinity (pink solid lines), dissolved oxygen (DO,  $\mu\text{mol kg}^{-1}$ ) (purple dots) and buoyancy frequency  $N^2$  ( $\text{s}^{-2}$ ) (bold black solid lines) at stations A8, A11, A14 and F304 (see Fig. 1b), with visits both pre-typhoon (Leg 1) and post-typhoon (Legs 2 and 3). The vertical distributions of  $N^2$  have been smoothed by the Gaussian method.

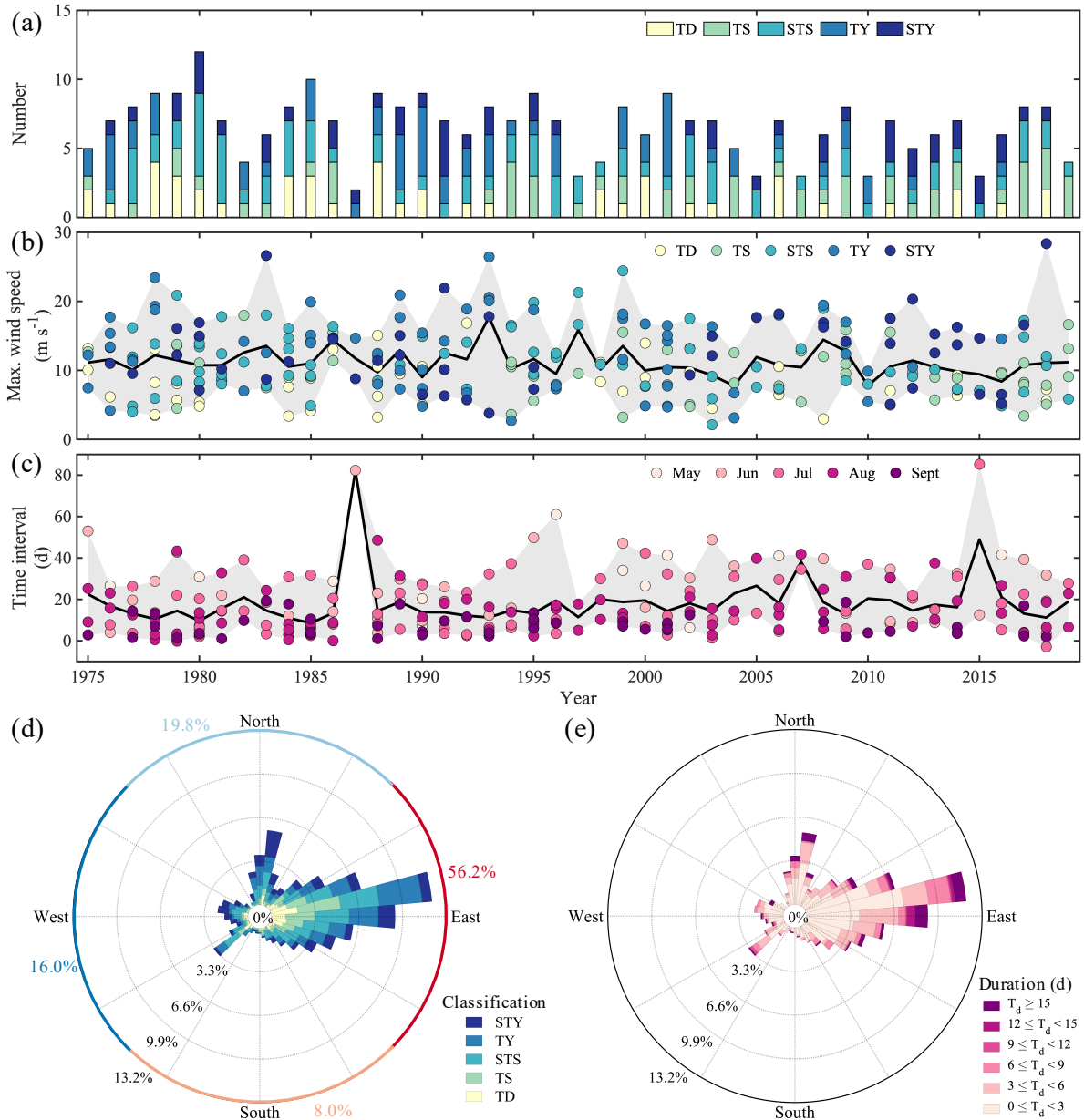


**Figure 4:** Statistics of tropical cyclones in the northern South China Sea (NSCS) from May to September over 1975-2019. (a) The number of tropical cyclones. TD, TS, STS, TY and STY represent tropical depressions (the maximum wind speed near the centre is between  $10.8\text{-}17.1 \text{ m s}^{-1}$  over its lifetime), tropical storms ( $17.2\text{-}24.4 \text{ m s}^{-1}$ ), strong tropical storms ( $24.5\text{-}32.6 \text{ m s}^{-1}$ ), typhoons ( $32.7\text{-}41.4 \text{ m s}^{-1}$ ) and strong typhoons ( $41.5\text{-}50.9 \text{ m s}^{-1}$ ), respectively. (b) The maximum wind speed of each tropical cyclone. The black line and grey shadow denote the annual average and range of the maximum wind speeds. (c) The time interval between two successive tropical cyclones. The black line and grey shadow denote the annual average and range of the time intervals. (d) The wind rose of the intensity of tropical cyclones. (e) The wind rose of the duration of tropical cyclones. The wind speed in (b) and wind direction in (d, e) were recorded at the Waglan Island station.

**Table 1:** Summary of annual mean numbers of tropical cyclones in each decade from 1950-2019. TD, TS, STS, TY and STY represent tropical depressions (the maximum wind speed near the centre is between 10.8-17.1 m s<sup>-1</sup> over its lifetime), tropical storms (17.2-24.4 m s<sup>-1</sup>), strong tropical storms (24.5-32.6 m s<sup>-1</sup>), typhoons (32.7-41.4 m s<sup>-1</sup>) and strong typhoons (41.5-50.9 m s<sup>-1</sup>), respectively.

Years	TD	TS	STS	TY	STY	SUM
1950-1959	3.5	1.1	1.2	1.1	1.5	8.4
1960-1969	1.7	0.6	1.5	2.1	2.7	8.6
1970-1979	1.8	0.7	2.1	2.1	1.2	7.9
1980-1989	1.5	0.7	2.5	1.3	1.3	7.3
1990-1999	0.7	1.2	1.8	2	1.1	6.8
2000-2009	0.9	1.4	1.5	1.5	0.8	6.1
2010-2019	0.6	1.8	1.4	0.4	1.5	5.7

### Specific comments

*L89: What are DIC and TA used for? How come you didn't use your DIC data to validate your estimate of OCR and to support your conclusions?*

**[Response]:** DIC and TA were used for validating the three-endmember mixing model. TA is a quasi-conservative parameter due to its small changes during biological processes. Comparing our predicted values with measured TA, we found they were consistent with a subtle difference of  $8 \pm 8 \mu\text{mol kg}^{-1}$  because of measurement errors, propagation of uncertainty through the mixing scheme and/or biological processes (Fig. 5b). DIC is produced with the oxygen depletion. We calculated the biochemical-induced DIC and DO changes for each leg and found that they had a good relationship with a slope of  $-0.93 \pm 0.07$  (Fig. 5c), similar to that reported by Zhao et al. (2020) for the same study area.

We agree with the reviewer that we should use the DIC data to validate our estimates of the OCR. We have calculated the biochemical-induced DIC changes ( $\Delta\text{DIC}^{\text{bc}}$ ) from Leg 2 to Leg 3, but uncertainties in DIC from the conservative mixing among three water masses reached  $\sim 30 \mu\text{mol kg}^{-1}$ , mainly due to a large variability in the DIC concentration of the brackish plume endmember (Table 2). These uncertainties were comparable to changes in DIC between two legs for nearly half of the sampling stations during Leg 3 (uncertainties in DO were only  $\sim 5 \mu\text{mol kg}^{-1}$ , much smaller than changes in the DO concentration from Leg 2 to Leg 3). We thus plotted the biochemical-induced DIC changes versus DO changes from Leg 2 to Leg 3, also showing a good relationship with a slope of  $-0.92 \pm 0.17$  (Fig. 2), to indirectly validate our estimates of the OCR. This slope was consistent through the sampling legs, implying aerobic respiration of organic matters indeed dominated the OCR.

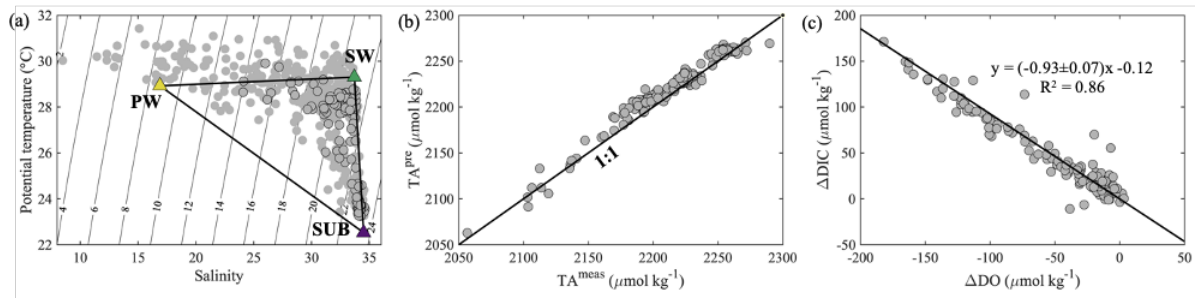


**Figure 5:** (a) Potential temperature (°C) vs. salinity, (b) predicted TA ( $TA^{pre}$ ,  $\mu\text{mol kg}^{-1}$ ) vs. measured TA ( $TA^{meas}$ ,  $\mu\text{mol kg}^{-1}$ ), and (c)  $\Delta\text{DIC}$  ( $\mu\text{mol kg}^{-1}$ ) vs.  $\Delta\text{DO}$  ( $\mu\text{mol kg}^{-1}$ ) on the NSCS shelf off the PRE. The black-edged circles represent bottom water samples with depths > 10 m. The yellow, green and purple triangles in (a) represent the endmember values of Brackish Plume Water (PW), offshore surface water (SW) and upwelled subsurface water (SUB), respectively. The black line in (c) denotes the slope of  $\Delta\text{DIC}$  plotted against  $\Delta\text{DO}$  derived from the Model II regression.

**Table 1:** Summary of end-member values adopted in the three-endmember mixing model

Water mass	$\theta$ (°C)	Salinity	DIC ( $\mu\text{mol kg}^{-1}$ )	DO ( $\mu\text{mol kg}^{-1}$ )
Brackish plume water	$28.9 \pm 0.4^b$	16.9	$1776 \pm 29^b$	$217.3 \pm 1.4^c$
Offshore surface water <sup>a</sup>	$29.3 \pm 0.1$	$33.7 \pm 0.1$	$1922 \pm 5$	$194.4 \pm 0.3^c$
Upwelled subsurface water <sup>a</sup>	$22.5 \pm 0.1$	$34.5 \pm 0.0$	$2022 \pm 3$	180.9

<sup>a</sup>Endmember values were adopted from Zhao et al. (2020)

<sup>b</sup>Uncertainties were derived from samples collected at the entrance of the PRE

<sup>c</sup>Uncertainties were calculated by propagating errors associated with the estimation of oxygen solubility using Benson and Krause Jr (1984)

*L101: did you collect chlorophyll samples? at what time of the day did you collect your chlorophyll profiles? did you notice non photochemical quenching near the surface and if so how did you correct the profiles?*

**[Response]:** We collected samples for chlorophyll *a* (Chl *a*) concentrations along with the cruise track during both day and night. We noticed the non-photochemical quenching near the surface from the fluorescence sensor, which was however not used to derive Chl *a*. Instead, we obtained the Chl *a* concentrations from discrete water samples. These samples were filtered onto GF/F (Whatman, USA) and stored in foil bags in liquid nitrogen until they were measured on a Trilogy laboratory fluorometer (Welschmeyer 1994) after extracted with 90% acetone for 14 h at -20 °C.

*Figure 1c: can you put shaded areas at the time of the cruises to be clear about the conditions during the sampling? Figure 1d: can you provide units and y-axis tick values? The length of the vectors don't seem to match the wind speed in the panel above. Also most vectors are oriented north-south and easterly winds vectors (associated with high wind speed) are small. Can you verify that the wind vectors are plotted properly?*

[Response]: We appreciate the suggestions. Accordingly, we have added shaded areas at the time of the cruises for each leg and re-plotted Figure 1d to match the arrow lengths with the wind speed (Fig. 6). During the cruise legs, easterly winds dominated with relatively larger east-west components than south-north components of wind velocities.

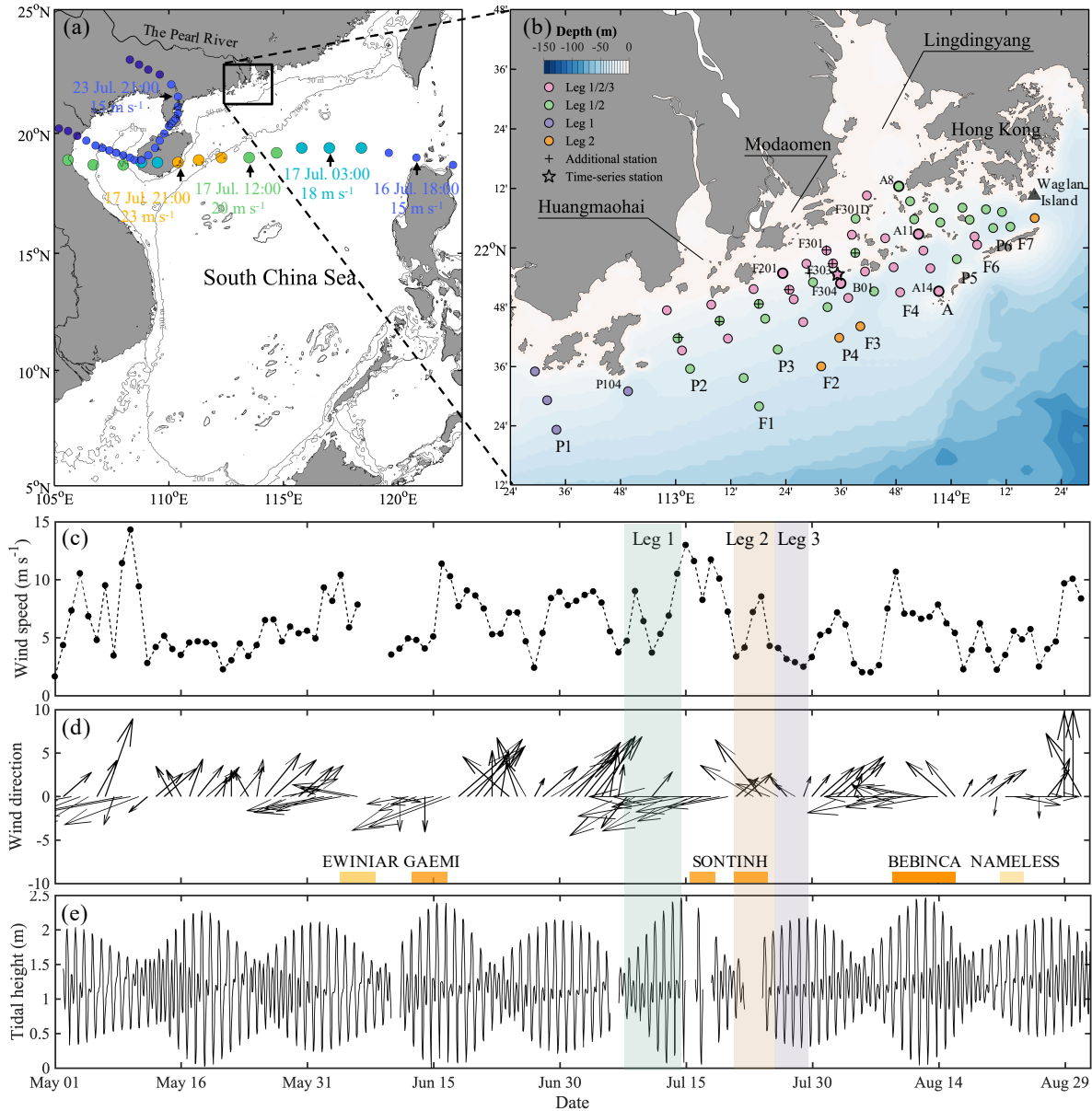


**Figure 6:** (a) Map of the study area on the northern South China Sea (NSCS) Shelf, showing the track of Typhoon SONTIHN (circles) across the NSCS during July 16-24, 2018. The color of the circles represents the magnitude of wind speed. Additionally, the smaller circles denote tropical depression (wind speeds  $\leq 17.1 \text{ m s}^{-1}$ ) and the larger circles denote tropical storm (wind speeds within  $17.2\text{-}32.6 \text{ m s}^{-1}$ ). The arrows denote the locations of the typhoon as marked with time and wind speed. The grey lines are the depth contours at 50 and 200 m. (b) Sampling stations on the NSCS shelf off the Pearl River Estuary in summer 2018. The pink, green, purple and orange circles denote stations surveyed in all three legs, only both Leg 1 and Leg 2, only Leg 1 and only Leg 2, respectively. Time-series observations were conducted at Station F303 as marked by the star, and vertically high-resolution samplings were conducted at stations marked with bold circles. (c) The wind speed and (d) wind direction at Waglan Island (triangle in (b)) from May to August, 2018. Bars at the bottom of (d) mark times when tropical cyclones impacted the NSCS. (e) The tidal height at the Dawanshan gauge station near Station F303 from May to August 2018.

August, 2018. The shaded area indicates the cruise periods for Leg 1 (grey), Leg 2 (pink) and Leg 3 (blue), respectively.

*L132: I have a hard time believing this assumption. Can you provide support to your claim?  
In Figure 3 bottom water conditions vary rapidly*

**[Response]:** We appreciate the reviewer's comment, which is indeed critical to this study. Please refer to our response to the general comment.

*Figure 3: This indicates the intrusion of warm/salty waters that participate to the re-stratification of the water column. What is the O<sub>2</sub> and OM content of these waters? is OCR driven by sediment O<sub>2</sub> consumption or just water column respiration? this figure indicates dynamic surface and bottom layers, not what it is described in the Results section (quiescent bottom layer). Do you know why O<sub>2</sub> increases near the bottom? is there an advective source of O<sub>2</sub> that is not taken into account?*

**[Response]:** We appreciate the critical comments. This figure indeed showed the intrusion of warm/salty waters, with the DO concentrations of  $\sim 180\text{-}184 \mu\text{mol kg}^{-1}$  and the POC concentrations of  $0.12\text{-}0.16 \text{ mg L}^{-1}$ , which differed by  $< 4 \mu\text{mol kg}^{-1}$  and  $< 0.04 \text{ mg L}^{-1}$ , respectively, from the upper waters. The estimated OCR here was mainly driven by water column respiration detailed in our response above.

We agree with the reviewer that the surface and bottom layers were dynamic over time, but with quite small variabilities (Fig. 1). As described in the Results section, the distribution of the DO concentrations in bottom layer was homogeneous and the distributions of temperature and salinity showed smaller cross-shore gradients than those during Leg 1, rather than quiescent. The slightly higher DO near the bottom layer likely resulted from previous strong vertical mixing upon disturbance by typhoon, which mixed high-DO surface waters into the depth. As the upward-intruded bottom waters in our time-series observations were warm but salty, and the DO distributions were almost homogeneous at the bottom layer during Leg 2 (Fig. 7), these bottom waters unlikely sourced from nearshore warm, less-salty waters or offshore cooler, saline waters via lateral advection. We thus contend that we have taken into account all advective sources of oxygen from Leg 2 to Leg 3.

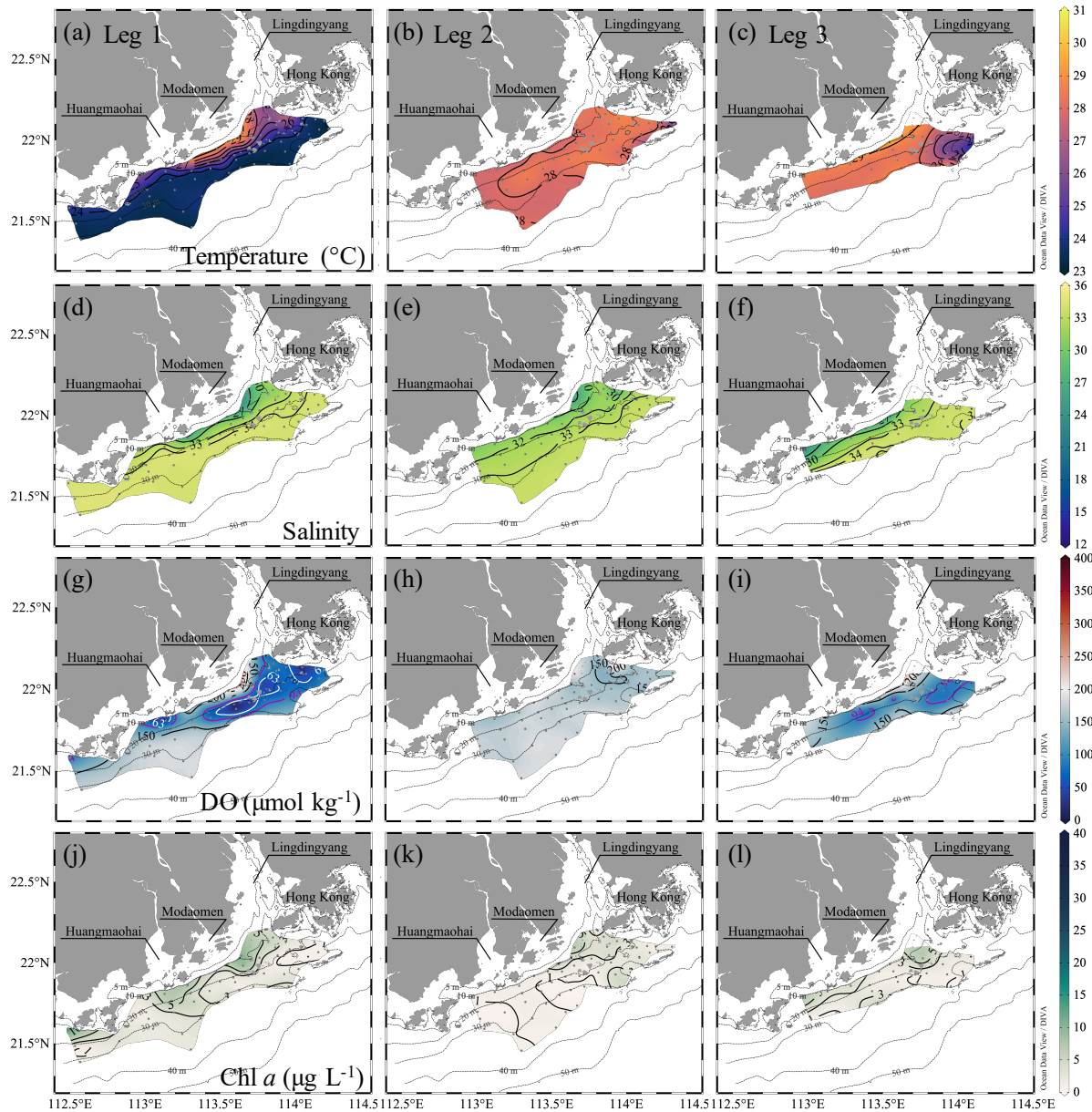


**Figure 7:** Distribution of temperature ( $^{\circ}\text{C}$ ), salinity, DO ( $\mu\text{mol kg}^{-1}$ ) and Chl *a* concentrations ( $\mu\text{g L}^{-1}$ ) at the bottom water layer off the PRE during Leg 1 pre-typhoon, and during Legs 2 and 3 post-typhoon. The white and magenta contours in (g) and (w) show the hypoxic ( $\text{DO} < 63 \mu\text{mol kg}^{-1}$ ) and oxygen-deficit ( $\text{DO} < 94 \mu\text{mol kg}^{-1}$ ) zones.

*L199: You should calculate stratification rather than citing others*

**[Response]:** We appreciate the suggestion. We calculated stratification using the buoyancy frequency, but we cannot partition the contributions from the vertical gradients in temperature or salinity. We cited the reference here supporting that vertical temperature gradients could intensify stratification in addition to vertical salinity gradients. We therefore would like to keep this citation as we will reorganize the paper to combine results and discussion into a clear narrative with an outline listed above in our response to the general comment.

*L200: it didn't shift westward but was advected offshore indeed*

**[Response]:** Accepted. Carefully comparing the surface salinity distributions during three legs, we will correct the statement as “The freshwater bulge of lower salinity ( $< 15$ ) advected offshore around the Modaomen sub-estuary” in our revised manuscript.

*L201: you are mixing discussion here*

**[Response]:** Accepted. We will reorganize the paper to combine results and discussion to a clear narrative with an outline as listed above in our response to the general comment, and also revise the statement as “... likely driven by the interaction between the seaward buoyant current and northeastward shelf current (Pan et al. 2014, Li et al. 2020)” in our revised manuscript.

*L241: but salinity (i.e. plume waters) will also control the wind intensity that is required to mix the water column*

**[Response]:** We agree with the reviewer that the wide-spreading plume also influences the wind-driven turbulent mixing. We discussed in sequence the effects of freshwater inputs (i.e., river plume), wind stress and direction, tidal fluctuations and spring-to-neap tidal oscillations on the water column stability. We therefore will correct the statement as “Water column stability also largely depends on wind stress in coastal waters” and discuss the effects of river plume vs. wind stress on the water column stability in our revised manuscript.

*L246: Figure 2j,n shows stratification during leg 2, i.e. surface plume water, so the vertically homogeneous water column occurs before leg 2 (July 14-19)*

**[Response]:** Accepted. We will correct the statement as “The strong winds mixed high-temperature, low-salinity surface waters and cold, saline bottom waters, resulting in a vertically-homogeneous temperature and salinity, as observed in the first half of the time-series observations before Leg 2” in our revised manuscript.

*L248: Figure 2l indicates a strong post-storm bloom that is not mentioned*

**[Response]:** We described the strong post-storm bloom in Section 3.2 — Destruction of hypoxia by typhoon — “Stronger blooms than that during Leg 1 were identified in the surface plume, widely spreading from the mouth of the Lingdingyang sub-estuary to near the Huangmaohai sub-estuary, potentially fueled by nutrients mixed upward from the deep in addition to riverine inputs (Wang et al. 2017, Qiu et al. 2019). The maximum Chl *a*

concentration was  $> 40 \mu\text{g L}^{-1}$  off the Modaomen sub-estuary, accompanied by an extraordinarily high DO concentration of  $> 350 \mu\text{mol kg}^{-1}$ ”.

*L253: This should be true along the coast where the plume is trapped but not offshore*

**[Response]:** We agree with the reviewer. Indeed, here we discussed the water column stability along the coast mostly within the 30-m isobaths where the plume was trapped.

*L254: This is discussed in a recent paper of the Changjiang estuary, you could have a look, I assume similar mechanisms occur in the PRE. <https://doi.org/10.5194/bg-2019-341>*

**[Response]:** We appreciate the suggestion. This paper discusses the effect of wind direction on the plume spreading (Zhang et al. 2020), which indirectly correlates the hypoxia extent to the wind direction: the strong northward wind redistributes and advects the river plume towards the Yangtze Bank through Ekman transport, while the weakened northward or westward wind allows the location of the bottom hypoxia to migrate to the Submarine Canyon (Zhang et al. 2019). Similarly, off the PRE, upwelling-favorable winds (i.e., southwesterly) could drive the river plume offshore and eastward (Gan et al. 2009), increasing the hypoxia area; but downwelling-favorable easterly winds tend to constrain the river plume near the coast and drive surface waters to penetrate into the depth (Fig. 7), leading to an offshore shift of the hypoxic zone within a limited area beneath the surface plume. If the easterly winds last for a longer time than the hypoxia timescale, stronger blooms in the surface plume would enhance the bottom hypoxia with an abundant supply of fresh, labile organic matters. Based on the above notions, we will revise the statement in our revised manuscript.

*L259: This is an interesting discussion but not supported by your observations so it feels a bit off topic*

**[Response]:** Accepted. We will revise this discussion by calculating the potential maximum area of  $\sim 990 \text{ km}^2$  and  $\sim 1930 \text{ km}^2$  for the hypoxic and oxygen-deficient zones, as spring-to-neap tidal oscillations lead to variations in the DO concentration with a maximum neighboring oxygen range of  $0.5 \text{ mg L}^{-1}$  (Cui et al. 2019) and our cruise legs were all conducted during the transformation from a neap tide to a spring tide (Fig. 6e). The hypoxia and oxygen-deficient areas therefore might be underestimated by at most of 34-50% in our sampling area due to tidal fluctuations.

*L291: what does that mean? that salinity was  $>xx$  in your samples?*

**[Response]:** The statement “we selected samples with water depths > 10 m, approximately below the pycnocline and where the surface plume was rarely involved” means that samples used for calculating the OCR were below the pycnocline and less affected by the upper plume waters. The selected samples with water depths > 10 m have salinity of > 31. We will revise the statement as “we selected samples with water depths > 10 m, approximately below the pycnocline and less affected by the upper plume waters” in our revised manuscript.

*L308: it is not a lower limit but an average estimate*

**[Response]:** The OCR was spatially averaged, but it was also a lower limit because we might overestimate the actual time for the significant oxygen consumption since its initiation between Leg 2 and Leg 3 and underestimate the diffusion of oxygen from the surface layer (assumed negligible during our estimates of the OCR), both of which likely underestimate the OCR.

*L309: I am surprised that there was no advective sources/sinks of O<sub>2</sub> given the observations in Figure 3*

**[Response]:** We admit that there were vertically advective sources/sinks of O<sub>2</sub> in the time-series observations (Fig. 1), but the upward intrusion of slightly warm/salty waters was progressively suppressed by the surface plume to the end of the time-series observations. We also observed the wide-spreading river plume at the surface layer during Leg 2 (Fig. 8), restoring the vertical stratification and restricting the oxygen supply from the surface layer. In addition, the slightly higher DO near the bottom layer likely resulted from previous strong vertical mixing upon disturbance by typhoon, which mixed high-DO surface waters into the depth. As the upward-intruded bottom waters in our time-series observations were warm but salty, and the DO distributions were almost homogeneous at the bottom layer during Leg 2 (Fig. 7), these bottom waters unlikely sourced from nearshore warm, less-salty waters or offshore cooler, saline waters via lateral advection. We thus contend that we have taken into account all advective sources of oxygen from Leg 2 to Leg 3.

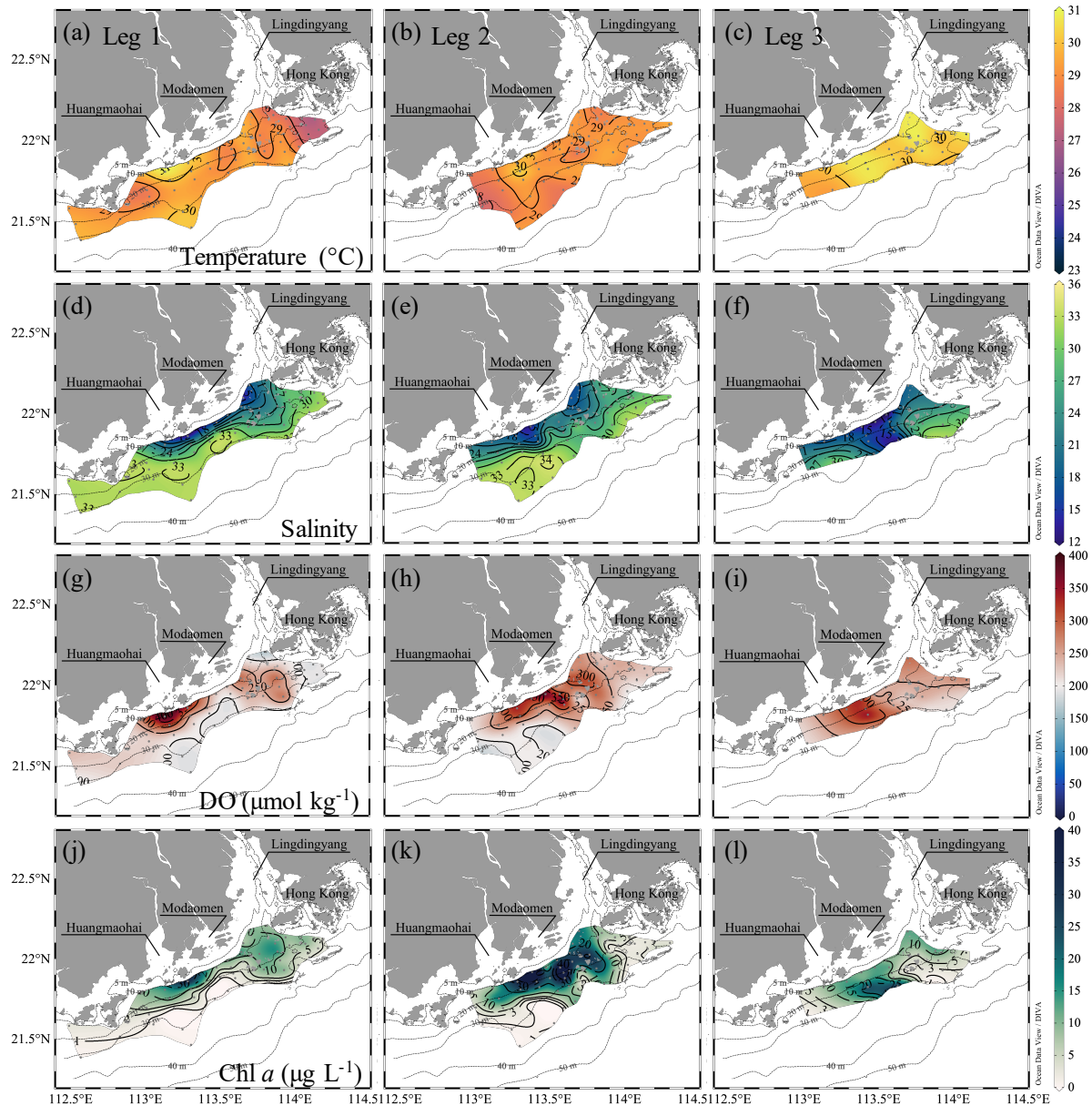


**Figure 8:** Distribution of temperature ( $^{\circ}\text{C}$ ), salinity, DO ( $\mu\text{mol kg}^{-1}$ ) and Chl *a* concentrations ( $\mu\text{g L}^{-1}$ ) at the surface water layer off the PRE during Leg 1 pre-typhoon, and during Legs 2 and 3 post-typhoon. The white and magenta contours in (g) and (w) show the hypoxic ( $\text{DO} < 63 \mu\text{mol kg}^{-1}$ ) and oxygen-deficit ( $\text{DO} < 94 \mu\text{mol kg}^{-1}$ ) zones. Figures were produced using Ocean Data View v. 5.3.0 (<http://odv.awi.de>, last access: 08 June 2020)

L313: You have to be clear how you use the terminology OCR. An increase in the OCR value (more positive) indicate a reoxygenation.

**[Response]:** We appreciate the critical comment. Changes in the OCR of a negative value were confusing. We will revise the definition for the OCR as the biochemical-induced DO consumption with time. A higher OCR value indicates stronger oxygen consumption and a negative value indicates oxygen production due to biochemical processes (e.g., photosynthesis). Accordingly, we will correct all the statements associated with changes in the OCR.

L314: where is this shown?

[Response]: The data were not shown in time series for explicit comparison. We have plotted the figure to show this data (Fig. 9) and will add this figure to our revised supplementary material.

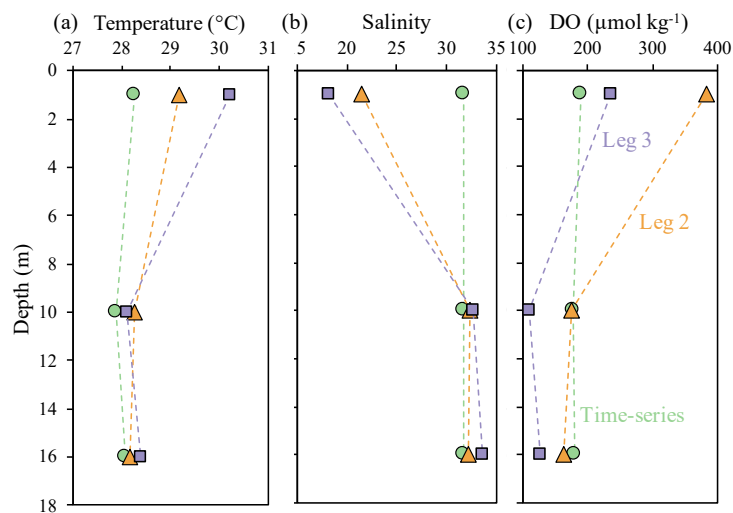


**Figure 9:** Profiles of temperature ( $^{\circ}\text{C}$ ), salinity and DO ( $\mu\text{mol kg}^{-1}$ ) at station F303 at the end of the time-series observations and during Leg 2 and Leg 3.

L315: "decreased": so you mean less negative?

[Response]: The reviewer is correct that the OCR was less negative as it varied from  $\sim -9 \mu\text{mol O}_2 \text{ kg d}^{-1}$  (July 20-22) to  $\sim -5.5 \mu\text{mol O}_2 \text{ kg d}^{-1}$  (July 22-29). To avoid misleading, we will revise the definition of the OCR as the biochemically-induced oxygen consumption with time. A higher OCR value indicates stronger oxygen consumption and a negative value indicates oxygen production due to biochemical processes (e.g., photosynthesis). We will also correct the statement as "DO declined at a rate of  $\sim 9 \mu\text{mol O}_2 \text{ kg}^{-1} \text{ d}^{-1}$  from July 20-22, when the winds remained strong, and the OCR decreased to  $\sim 5.5 \mu\text{mol O}_2 \text{ kg}^{-1} \text{ d}^{-1}$  from Leg 2 to Leg 3 (from July 22-29)" in our revised manuscript.

L317: you mean horizontal diffusion?

[Response]: The reviewer is correct, but we found that the horizontal diffusion for oxygen between the hypoxic zone and its surrounding environment might be much smaller than that induced by lateral advection. We thus will revise it to solely discuss the lateral advection.

L316-320: your analysis is not well supported, can you discuss your results and be more quantitative? If not, please do not extrapolate

[Response]: We agree with the reviewer that the horizontal diffusion for oxygen was hypothetical and we will remove this discussion in our revised manuscript.

L324: Figure 3 indicates the intrusion of warm and salty subsurface waters at station F303 after the typhoon, can you comment on that and how it fits with your analysis?

[Response]: We appreciate the critical comment. Indeed, the time-series observations at station F303 indicated an upward intrusion of warm and salty subsurface waters (Fig. 1), but this upward intrusion was progressively suppressed by the surface plume. The water column below the pycnocline became almost vertically well-mixed to the end of the time-series observations before Leg 2, showing small vertical variabilities in profiles of temperature, salinity and DO concentrations. Therefore, this upward-intrusion before Leg 2 will not compromise our assumption for estimating the OCR from Leg 2 to Leg 3.

Specifically, we attributed the upward intrusion to the subdued vertical mixing due to weakened winds (Fig. 6c), resulting in a less well-mixed water column. The upward-intruded warm and salty waters (temperature > 28.1 °C and salinity > 32.2) resulted from the antecedent strong winds-induced vertical mixing upon disturbance by typhoon, which mixed the warm, brackish surface waters (> 29 °C; Fig. 8a) downward to increase the temperature of bottom waters. Indeed, the bottom waters were > 28.1 °C with water depths > 16 m (the depth of the bottom layer at station F303) during Leg 2 (Fig. 7). The relatively cooler surface waters might result from the heat loss at the air-sea interface due to the reduction in air temperature by ~ 2-3 °C during the typhoon period and afterwards (Fig. 10).

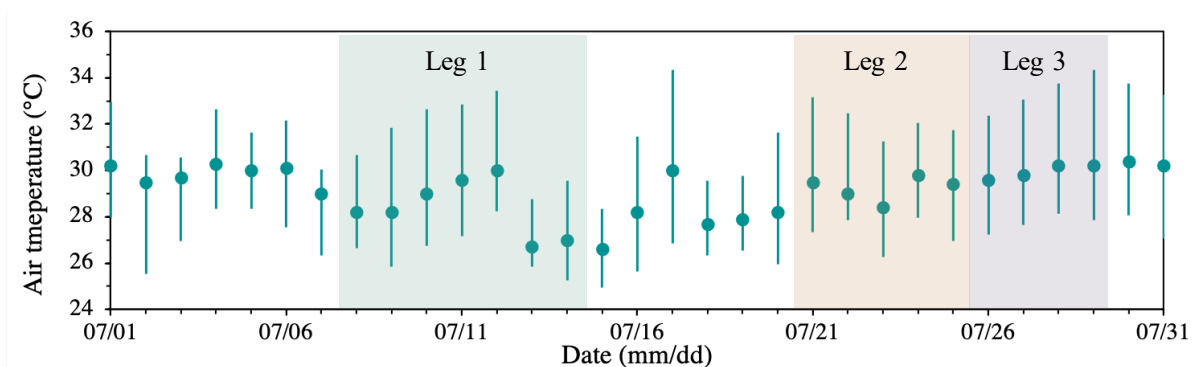


**Figure 10:** The air temperature at the Hong Kong Observatory in July 2018. The shaded area indicates the cruise periods for Leg 1 (grey), Leg 2 (pink) and Leg 3 (blue), respectively.

L336: end of sentence: (Figure 5)

[Response]: Accepted. We will add the reference of the figure at the end of the sentence.

L338: those are really rough estimates. It is impossible to see what are the bottom  $O_2$  values in Figure 2 so it is difficult to judge your reasoning. Is the  $OCR = -15$  value an average over the sampling area? bottom  $O_2$  values seem rather low over the entire area sampled during Leg 3

[Response]: We agree with the reviewer that it was a first order estimate for scaling to a larger area. This larger area implied the oxygen-deficient zone which likely developed into the hypoxic zone off the PRE. Therefore, we used the OCR of  $\sim 15 \mu\text{mol O}_2 \text{ kg}^{-1} \text{ d}^{-1}$  averaged over the oxygen-deficient zone ( $\text{DO} < 94 \mu\text{mol kg}^{-1}$ ) during Leg 3, not over the whole sampling area. Despite low bottom oxygen values over the entire area during Leg 3, we showed relatively large spatial gradients of the total DO changes in bottom waters from Leg 2 to Leg 3 in Fig. 11. The pattern of the OCR was almost consistent with the total DO changes, due to much smaller mixing-induced DO changes than the total DO changes. We also have improved the quality of figures by enlarging labels and boldening lines (Fig. 7) for a better judgement on our reasoning.

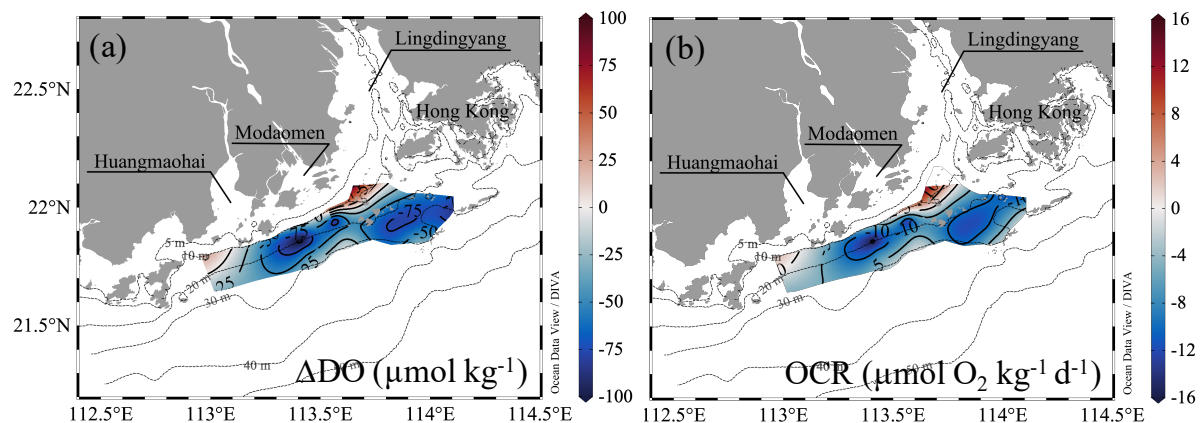


**Figure 11:** Distribution of (a) total DO changes ( $\Delta\text{DO}$ ,  $\mu\text{mol kg}^{-1}$ ) and (b) the biochemical-induced oxygen consumption rate (OCR,  $\mu\text{mol O}_2 \text{ kg}^{-1} \text{ d}^{-1}$ ) between Leg 3 and Leg 2 on the inner NSCS shelf off the PRE.

L341: Figure 3 shows that this is more variable than assumed here

[Response]: We agree with the reviewer that the time-series observations showed slightly more variable, because the time-series observations were conducted after the passage of the typhoon but still with relatively strong winds decreasing from  $\sim 10 \text{ m s}^{-1}$  to  $\sim 7 \text{ m s}^{-1}$  (Fig. 6c). The upward intrusion of warm and salty bottom waters was also progressively suppressed by the freshwater input-induced stratification to the end of the time-series observations (Fig. 1). This would not conflict with our assumption here for a common scenario during the late spring, typically with a monthly average wind speed of  $< 6 \text{ m s}^{-1}$ . The subsurface waters below the pycnocline therefore could be assumed almost well-mixed.

*L345: how did you come up to the value 183 from your assumption? do you assume mixing rather than water replacement during intrusion?*

**[Response]:** Thanks for the critical comment. Based on our assumption, the well-oxygenated offshore surface waters have an DO concentration of  $\sim 194 \mu\text{mol kg}^{-1}$ . We also estimated that shoreward-intruded subsurface waters reduced the initial DO level by  $8.6 \pm 1.7\%$  of the oxygen decline for hypoxia formation —  $\sim 11 \mu\text{mol kg}^{-1}$  when the oxygen level decreased from  $\sim 194 \mu\text{mol kg}^{-1}$  to the threshold of hypoxia ( $63 \mu\text{mol kg}^{-1}$ ). The initial DO level for the biochemical-induced oxygen consumption for hypoxia formation was therefore  $\sim 183 \mu\text{mol kg}^{-1}$ . Actually, we assumed water mass mixing rather than water replacement during intrusion.

*L346: This does not match your calculation above with the average OCR, why are you assuming the maximum OCR during spring?*

**[Response]:** We appreciate the critical comment. We used the maximum OCR during the late spring to estimate a minimum time for the occurrence of hypoxia hotspots after the initiation of significant oxygen depletion. If the hypoxic zone develops to a larger spatial coverage, the time would be longer than the minimum time, which was consistent with our above estimates for the reinstatement of hypoxia in the summer of 2018.

*L347: you should compare your values with similar systems, i.e. river-dominated estuaries (8-89 days). Also you could discuss your estimates in comparison of the PRE values provided in the reference.*

**[Response]:** Accepted. We will compare our OCR estimates with previous studies in this study area and other large river-dominated shelf systems: “This result is larger than that estimated by Fennel and Testa (2019) — 4 days — using the modelled OCR of  $\sim 34 \mu\text{mol O}_2 \text{ kg}^{-1} \text{ d}^{-1}$  in the water column with a sediment oxygen demand of  $\sim 2.1 \text{ g m}^{-2} \text{ d}^{-1}$ , which were only applicable to the hypoxia formation in the Lingdingyang sub-estuary with shallower waters ( $\sim 5 \text{ m}$ ) (Zhang and Li 2010). This result is still at the lower end of the hypoxia timescale in large river-dominated shelves globally (e.g., East China Sea off the Changjiang estuary, Northern Gulf of Mexico and Northwestern Black Sea), which varies from 8 to 89 days for hypoxia to develop once initiated (Fennel and Testa 2019). This short hypoxia timescale likely owes to a high OCR in relatively warm subsurface waters fuelled by abundant labile organic matters (Su et al. 2017, Zhao et al. 2020)” in our revised manuscript.

*L368-403: The last 2 paragraphs are not related to your results*

**[Response]:** Accepted. We will revise these paragraphs by (1) checking the precipitation and river discharge after the typhoon, (2) correlating our discussion closely with our observations of stronger post-storm blooms and their offshore advection along with the river plume, and (3) estimating changes in the frequency and intensity of tropical cyclones and the time interval between two successive tropical cyclones during the wet seasons, to discuss about the evolution of hypoxia upon disturbance by tropical cyclones and its response to changes in the frequency and intensity of tropical cyclone activities.

*L368: You did not mention/discussed the phytoplankton bloom in leg 2*

**[Response]:** As responded above, we described the strong post-storm blooms in Section 3.2 — Destruction of hypoxia by typhoon. We will further discuss the response of the post-storm hypoxia development to tropical cyclone activities, which might largely depend on the dynamics of the strong post-storm blooms: “Enhanced vertical mixing and/or freshwater discharge supplied large amounts of nutrients to the surface layer to fuel phytoplankton blooms following large storms (Zhao et al. 2009, Ni et al. 2016, Wang et al. 2017), as shown in Fig. 3 that strong blooms occurred in the surface plume along the coast with much higher Chl *a* concentrations during Leg 2 than that during Leg 1. The fresh autochthonous organic matter, together with the resuspended sedimentary organic carbon, provides sufficient substrates for microbial respiration in a re-stratified water column, leading to renewed or even exacerbated bottom water oxygen depletion (Zhou et al. 2012, Song et al. 2020)”.

*L379: why?*

**[Response]:** The statement was confusing and hypothetical. We will revise the statement based on our observations — “Whether it can develop into more severe hypoxia compared to that found initially during Leg 1 depends on the net OCR and water column stability, up until the passage of the next storm, Typhoon BEBINCA (Fig. 1d)” — because the post-storm blooms advected offshore might reduce the downward transport of labile organic matters to fuel the oxygen depletion in the subsurface waters.

*Figure 6: I am not sure that annual averages are very pertinent, an average value per event might be more useful. For wind direction this could be presented as a pie chart. For wind speed, the time series is not very informative, may be think about an other way of presenting the results. This is somewhat included in Figure 6a but it would be interesting to know what is the maximum time between wind events for each year (or have some statistics based on your*

estimate of OCR). Also remember that hypoxia did not occur for most of the period shown here. panel c: please see comment regarding wind vectors in Figure 1, make sure those are right

**[Response]:** We appreciate the critical comments and constructive suggestions. The annual average was actually the annual average of the maximum local wind velocity for each tropical cyclone in the NSCS. We have revised the figure to additionally show the maximum wind speed of each tropical cyclone (Fig. 4b). For wind direction, we re-plotted it as roses of winds with the classifications of storm intensities and the duration times of tropical cyclones in the northern South China Sea (NSCS) (Fig. 4d, e). We also have calculated the time interval between two successive tropical cyclones for each year (Fig. 4c). In our calculations and statistics on historical tropical cyclones, only tropical cyclones that impacted the NSCS from May to September were taken into account because hypoxia often occurred from late spring to summer and disappeared in autumn in this study area.

L398: *it depends on the direction, offshore intrusions would presumably bring lower O<sub>2</sub> waters*

**[Response]:** We agree with the reviewer that offshore intrusions would bring lower-oxygen waters due to the deoxygenation of oceanic waters and it might contribute to the oxygen loss for the formation of hypoxia more significantly, but we will remove this statement as it was less related to our topic.

L409: *"lowest ever recorded"*

**[Response]:** Accepted. We will correct the statement as “Eutrophication-induced hypoxia off the PRE was exacerbated with an enlarged area of ~ 660 km<sup>2</sup> and the lowest ever recorded regional DO concentration of 3.5 μmol kg<sup>-1</sup> (~ 0.1 mg L<sup>-1</sup>)” in our revised manuscript.

L417: *This is speculation, higher discharge may lead to lower nutrient concentrations in river waters, more export to deep areas where hypoxia does not occur*

**[Response]:** We agree with the reviewer that the higher discharge may decrease nutrient concentrations in river waters, but the total discharge of nutrients may increase due to strong flushing (Guo et al. 2008). In this study, stronger blooms occurred during Leg 2 than that during Leg 1, significantly utilizing the nutrients and producing organic matters to fuel the oxygen depletion in the subsurface waters. However, we observed an offshore shift of the blooms along with the river plume during Leg 3. Therefore, whether more nutrients will export to deep areas also depends on the phytoplankton uptake, the wind direction and alongshore currents that drive the river plume to spread offshore and their dominance on the water residence time. We will revise this statement without nutrient loading in our revised manuscript.

**Minor comments/edits:**

*L80: can you provide the number of stations in parenthesis for each leg, it is difficult to estimate it from Figure 1b*

**[Response]:** Accepted. We will add the number of stations for each leg as “Almost all stations in Leg 1 (56 stations) were revisited during Leg 2 (56 stations, including 4 stations differing from Leg 1), and nearly half again during Leg 3 (27 stations)” in our revised manuscript.

*L81: suggestion: "on the way back to port"*

**[Response]:** Accepted. We will revise the statement as “Eight stations were additionally revisited on the way back to the port on July 31” in our revised manuscript.

*L155-164: You are mixing results and discussion*

**[Response]:** Accepted. We will reorganize the paper to combine results and discussions to a clear narrative with an outline listed above in our response to the general comment. Therefore, we kept them and will further compare the results with that in the summer of 2014 (Su et al. 2017).

*Figure 2: there is no point showing the river labels, they are way too small. Also the contour labels cannot be seen and the color bars are way too small. I suggest you move the colorbar to the top of each column and make it thicker with larger fonts An alternative suggestion is to split the figure into surface and bottom figures and flip the rows to columns to make larger panels*

**[Response]:** Accepted. Accordingly, we have added the river label in Fig. 6a and separated this figure into two figures showing the surface and bottom distributions, respectively (Fig. 7 and Fig. 8). We also have enlarged the panels and contour labels for all figures.

*Figure 4: The labels and lines are very small*

**[Response]:** Accepted. We have enlarged the labels and boldened the lines (Fig. 3).

*L312: not clear, the sentence should be rephrased*

**[Response]:** Accepted. We will rephrase the sentence as “During the hypoxia formation, the DO concentrations are in a non-steady state as oxygen sinks exceed sources. To shift towards a balance between oxygen consumption and replenishment for the maintenance of hypoxia, the OCR might decrease or the physical-induced oxygen supply increases.”

## References

- Benson, B. B. and Krause Jr, D.: The concentration and isotopic fractionation of oxygen dissolved in freshwater and seawater in equilibrium with the atmosphere<sup>1</sup>, *Limnol Oceanogr*, 29, 620-632, doi:10.4319/lo.1984.29.3.0620, 1984.
- Cui, Y. S., Wu, J. X., Ren, J. and Xu, J.: Physical dynamics structures and oxygen budget of summer hypoxia in the Pearl River Estuary, *Limnol Oceanogr*, 64, 131-148, doi:10.1002/lno.11025, 2019.
- Fennel, K. and Testa, J. M.: Biogeochemical Controls on Coastal Hypoxia, *Annual Review of Marine Science*, 11, 105-130, doi:10.1146/annurev-marine-010318-095138, 2019.
- Gan, J. P., Li, L., Wang, D. X. and Guo, X. G.: Interaction of a river plume with coastal upwelling in the northeastern South China Sea, *Cont Shelf Res*, 29, 728-740, doi:10.1016/j.csr.2008.12.002, 2009.
- Guo, X. H., Cai, W. J., Zhai, W. D., Dai, M. H., Wang, Y. C. and Chen, B. S.: Seasonal variations in the inorganic carbon system in the Pearl River (Zhujiang) estuary, *Cont Shelf Res*, 28, 1424-1434, doi:10.1016/j.csr.2007.07.011, 2008.
- Kemp, W. M., Sampou, P. A., Garber, J., Tuttle, J. and Boynton, W. R.: Seasonal depletion of oxygen from bottom waters of Chesapeake Bay: roles of benthic and planktonic respiration and physical exchange processes, *Mar Ecol Prog Ser*, 85, 137-152, 1992.
- Li, D., Gan, J., Hui, R., Liu, Z., Yu, L., Lu, Z. and Dai, M.: Vortex and Biogeochemical Dynamics for the Hypoxia Formation Within the Coastal Transition Zone off the Pearl River Estuary, *Journal of Geophysical Research: Oceans*, 125, e2020JC016178, doi:10.1029/2020JC016178, 2020.
- Lu, Z. M., Gan, J. P., Dai, M. H., Liu, H. B. and Zhao, X. Z.: Joint Effects of Extrinsic Biophysical Fluxes and Intrinsic Hydrodynamics on the Formation of Hypoxia West off the Pearl River Estuary, *J Geophys Res-Oceans*, 123, 6241-6259, doi:10.1029/2018jc014199, 2018.
- Pan, J. Y., Gu, Y. Z. and Wang, D. X.: Observations and numerical modeling of the Pearl River plume in summer season, *J Geophys Res-Oceans*, 119, 2480-2500, doi:10.1002/2013jc009042, 2014.
- Qiu, D., Zhong, Y., Chen, Y., Tan, Y., Song, X. and Huang, L.: Short-Term Phytoplankton Dynamics During Typhoon Season in and Near the Pearl River Estuary, South China Sea, *Journal of Geophysical Research: Biogeosciences*, 124, 274-292, doi:10.1029/2018JG004672, 2019.
- Su, J. Z., Dai, M. H., He, B. Y., Wang, L. F., Gan, J. P., Guo, X. H., Zhao, H. D. and Yu, F. L.: Tracing the origin of the oxygen-consuming organic matter in the hypoxic zone in a large eutrophic estuary: the lower reach of the Pearl River Estuary, China, *Biogeosciences*, 14, 4085-4099, doi:10.5194/bg-14-4085-2017, 2017.

Wang, B., Hu, J. T., Li, S. Y. and Liu, D. H.: A numerical analysis of biogeochemical controls with physical modulation on hypoxia during summer in the Pearl River estuary, *Biogeosciences*, 14, 2979-2999, doi:10.5194/bg-14-2979-2017, 2017.

Welschmeyer, N. A.: Fluorometric analysis of chlorophyll a in the presence of chlorophyll b and pheopigments, *Limnol Oceanogr*, 39, 1985-1992, doi:10.4319/lo.1994.39.8.1985, 1994.

Zhang, H., Fennel, K., Laurent, A. and Bian, C.: A numerical model study of the main factors contributing to hypoxia and its interannual and short-term variability in the East China Sea, *Biogeosciences*, 17, 5745-5761, doi:10.5194/bg-17-5745-2020, 2020.

Zhang, H. and Li, S. Y.: Effects of physical and biochemical processes on the dissolved oxygen budget for the Pearl River Estuary during summer, *J Marine Syst*, 79, 65-88, doi:10.1016/j.jmarsys.2009.07.002, 2010.

Zhang, W., Wu, H., Hetland, R. D. and Zhu, Z.: On Mechanisms Controlling the Seasonal Hypoxia Hot Spots off the Changjiang River Estuary, *Journal of Geophysical Research: Oceans*, 124, 8683-8700, doi:10.1029/2019jc015322, 2019.

Zhao, Y., Liu, J., Uthairan, K., Song, X., Xu, Y., He, B., Liu, H., Gan, J. and Dai, M.: Dynamics of inorganic carbon and pH in a large subtropical continental shelf system: Interaction between eutrophication, hypoxia, and ocean acidification, *Limnol Oceanogr*, 65, 1359-1379, doi:10.1002/lno.11393, 2020.